Anomalous population of ^{10}He states in reactions with ^{11}Li

P.G. Sharov,[1,2] I.A. Egorova,[3,2] and L.V. Grigorenko[1,4,5]

[1] *Flerov Laboratory of Nuclear Reactions, JINR, Dubna, RU-141980 Russia*
[2] *SSC RF ITEP of NRC "Kurchatov Institute", Moscow RU-117218 Russia*
[3] *Bogoliubov Laboratory of Theoretical Physics, JINR, Dubna, RU-141980 Russia*
[4] *GSI Helmholtzzentrum für Schwerionenforschung, Planckstraße 1, D-64291 Darmstadt, Germany*
[5] *National Research Center "Kurchatov Institute", Kurchatov sq. 1, RU-123182 Moscow, Russia*

(Dated: March 10, 2014.)

Structure with the lowest energy observed in the ^{10}He spectrum populated in the proton knockout reaction with ^{11}Li beam has a peak at $1.2-1.5$ MeV. This peak is usually interpreted as a resonant 0^+ ground state of ^{10}He. Our theoretical calculations indicate that this peak is likely to be a pileup of 1^-, 0^+, and 2^+ excitations with very similar shapes. Moreover, the "soft" 1^- excitation appears to be the lowest one in energy. Such an anomalous continuum response is traced to the halo structure of ^{11}Li providing extreme low energy shift to all the expected continuum excitations. Competitions of the initial state structure (ISS) and the final state interaction (FSI) effects on the spectrum and three-body correlations in ^{10}He are discussed. Analogous effect of the extreme low-energy shift could also be expected in other cases of $2n$ emitters populated in reactions with halo nuclei. Simplified example of the ^{10}He spectrum in α knockout from ^{14}Be, is given. We also discuss limits on the properties of ^{9}He stemming from the observed ^{10}He spectrum.

PACS numbers: 24.50.+g, 24.70.+s, 25.45.Hi, 27.20.+n

arXiv:1403.1748v1 [nucl-th] 7 Mar 2014

I. INTRODUCTION

The dripline systems often represent complicated and unusual forms of nuclear structure. These include nucleon halos, soft continuum excitation modes, abnormal cross sections for certain reactions. The ^{10}He nucleus has one of the largest known N/Z ratio representing the extreme situation of the nuclear matter asymmetry. This system is very complicated for studies and due to neutron excess there are only few realistic methods to populate states in this interesting nuclear system.

Since the experimental discovery of ^{10}He in 1994 [1] there were only several experimental studies [2–7]. Among the available experimental data on ^{10}He we would like to skip the discussion of two results [2, 3] which are complicated for interpretation. Then we end with two "lines" of research which we can consider as well established results. (i) Low-lying peak in the ^{10}He spectrum was observed in knockout reactions from halo nuclei: from ^{11}Li in Ref. [1] providing $E_T = 1.2(3)$ MeV, from ^{11}Li in Ref. [5] providing $E_T = 1.4 - 1.5$ MeV, $\Gamma \sim 1.9$ MeV, and from ^{14}Be (α or $2p$ removal [7]) giving $E_T = 1.60(25)$ MeV, $\Gamma = 1.8(4)$ MeV. It should be noted that the low-lying spectra in all these experiments are practically identical, although the details of data interpretation are different. We demonstrate in this work that it could be more than just a coincidence. (ii) ^{10}He spectrum was populated by the ^{3}H(^{8}He,p) two-neutron transfer reaction in two consequent works [4, 6]. In Ref. [6] the cross section peak with $E_T = 2.1(2)$ MeV and $\Gamma \sim 2$ MeV was observed. Also an evidence was obtained in this work for anomalous $\{0^+, 1^-, 2^+\}$ level ordering in ^{10}He. The earlier experiment [4] has a very limited statistics to give a quantitative result, but the conclusion, that there is no indication of a resonant ^{10}He state at about $1.0 - 1.5$ MeV, is valid in both works. Thus for the first glance there is a contradiction between two types of the data.

Theoretical results on ^{10}He are also sparse. The ^{10}He ground state structure and decay were studied in papers [8–10] providing results in generally consistent, but with a lot of differences in details. In Ref. [10] broad exploratory studies of the ^{10}He g.s. population were performed in the framework of the cluster ^{8}He+n+n model. The situation with interactions in the ^{8}He+n channel was quite uncertain at that moment due to controversial experimental data. This led to uncertain calculation results and essential freedom in interpretations. From theoretical point of view the calculations of ^{10}He spectrum is a reflection of the ^{9}He low-lying spectrum properties. Since that time we have got a confidence that in reality the spectrum of ^{10}He could be used to impose limitations on the spectrum of ^{9}He. This can be made, however, only if the understanding of the reaction mechanisms leading to population of ^{10}He is achieved.

Already in the paper [10] it was mentioned about the possible importance initial state effects for population of the ^{10}He in reactions with ^{11}Li. In paper [6] we extended qualitative calculations of Ref. [10] to the ^{10}He excitations with different J^π populated in transfer reactions providing explanation for experimental data [6]. Extension of our calculations for population of ^{10}He excitations with different J^π in the knockout reactions required considerably more effort and provided quite unusual results which we report here. These results well explain the above mentioned contradiction in the two types of data. They demonstrate potential danger of simple-minded attitude to interpretation of reaction data with exotic nuclei and promote the importance of a careful theoretical assessment.

II. SUDDEN REMOVAL OF PROTON AND THREE-BODY MODEL

In this work we report a large qualitative effect and we presume that even relatively simple reaction model — sudden removal of a proton — is sufficient at this stage. The model for sudden removal of a proton from ^{11}Li populating three-body ^{10}He continuum can be reformulated as a solution of the inhomogeneous three-body Schrödinger equation

$$(\hat{H}_3 - E_T)\Psi^{JM(+)}_{E_T}(X,Y) = \Phi^{JM}_q(X,Y). \qquad (1)$$

In this work we rely on the three-cluster ^{8}He+n+n model of ^{10}He and on the set of ^{8}He-n potentials developed in Ref. [10]. These potentials give a purely repulsive s-wave with $a_s \approx 3$ fm and the $p_{1/2}$ ground state of ^{9}He at 2 MeV and the $d_{5/2}$ state at about 5 MeV (the properties of the ^{9}He resonant states are those found in Ref. [11]). The justification for this choice is provided in Section VII.

In our theoretical approach the cross section for population of the three-body continuum is proportional to flux defined via WF with outgoing wave asymptotic:

$$\frac{d\sigma}{dE_T} \sim j(E_T) = \frac{1}{M}\, Im \int d\Omega_5 \Psi^{(+)\dagger}_{E_T} \rho^{5/2} \frac{d}{d\rho} \rho^{5/2} \Psi^{(+)}_{E_T} \Big|_{\rho_{\max}} .$$

The three-body ^{10}He WF $\Psi^{(+)}_{E_T}$ found in the hyperspherical harmonic method, depends either of hyperspherical variables $\{\rho, \Omega_5\}$, see Ref. [10] for details, or on the equivalent set of the Jacobi vectors $\{\mathbf{X}, \mathbf{Y}\}$, see Fig. 1.

To define the source function $\Phi^{JM}_q(X,Y)$ we use the cluster ^{11}Li WF in the form

$$\Psi^{J_i M_i}_{^{11}\mathrm{Li}}(\mathbf{X}, \mathbf{Y}', \mathbf{r}'_p) = [\Psi^{(3b)}_{^{11}\mathrm{Li}}(\mathbf{X}, \mathbf{Y}') \otimes \Psi_{^9\mathrm{Li}}(\mathbf{r}'_p)]_{J_i M_i}\,, \quad (2)$$

combining the three-body cluster WF of ^{11}Li $\Psi^{(3b)}_{^{11}\mathrm{Li}}$ with the single particle WF of the proton motion within the ^{9}Li cluster $\Psi_{^9\mathrm{Li}}$. The three-body WF is taken from paper [12] where it is constructed in the analytical Ansatz by fitting various observables to the available experimental data. We used the simplest form of the WF from [12] (without coupling to the spin on the core).

The p-wave ^{8}He+p WF $\Psi_{^9\mathrm{Li}}(\mathbf{r}'_p)$ is constructed in the potential model. We use the Woods-Saxon potential with the depth -56 MeV radius 3.03 fm and diffuseness 0.75 fm. It provides experimental binding energy for proton ^{9}Li ($E_b = 13.933$ MeV) and root mean square (rms) radius $\langle r'_p \rangle = 2.89$ fm, which allows to reproduce the rms matter radius of ^{9}Li with experimental rms matter radius of the ^{8}He cluster. The momentum space representation namely the squared formfactor of p+^{8}He WF is illustrated in Fig. 2.

Illustration of the reaction mechanism and relevant variables is provided by Fig. 1. In the initial coordinate system the sudden removal of proton from ^{9}Li core lead to momentum transfer to the ^{8}He cluster of the ^{9}Li

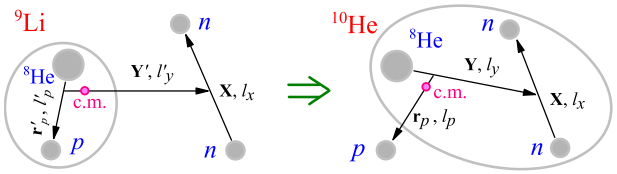

FIG. 1. The coordinate schemes used for proton removal (cluster removal in the general case) calculations.

core. To define the effect of such a momentum transfer on the whole final WF of ^{10}He we perform the coordinate transformation $\{\mathbf{Y}', \mathbf{r}'_p\} \to \{\mathbf{Y}, \mathbf{r}_p\}$ of WF (2). This is accomplished by decomposition of $\Psi^{J_i M_i}_{^{11}\mathrm{Li}}$ over hyperspherical harmonics for fixed X and l_x values of the two neutron subsystem and use of the Raynal-Revai transformation [13]. This transformation leads to WF in which proton coordinate is connected with the whole system (^{10}He) center-of-mass. In new coordinates $\{\mathbf{Y}, \mathbf{r}_p\}$ the source term for ^{10}He production is provided by acting on the proton by the annihilation operator. In coordinate space this operation gives

$$\Phi_{\mathbf{q}}(\mathbf{X}, \mathbf{Y}) = \int d^3\mathbf{r}_p e^{i\mathbf{q}\mathbf{r}_p} \Psi_{^{11}\mathrm{Li}}(\mathbf{X}, \mathbf{Y}, \mathbf{r}_p). \qquad (3)$$

The source functions for different J^π in ^{10}He are obtained by angular momentum decomposition

$$\Phi^{JM}_{q,\gamma,l_p}(X,Y) = \int d\Omega_x d\Omega_y d\Omega_q\, \Phi_{\mathbf{q}}(\mathbf{X}, \mathbf{Y})$$
$$\times [[[Y_{l_x}(\hat{X}) \otimes Y_{l_y}(\hat{Y})]_L \otimes \chi_S]_J \otimes Y_{l_p}(\hat{q})]_{JM}. \qquad (4)$$

The multi-index $\gamma = \{LSl_x l_y\}$ defines the complete set of angular quantum numbers for the core+N+N three-body problem.

For exploratory model calculations we also use the sources defined by the simple analytical expression:

$$\Phi^{JM}_{q,\gamma}(X,Y) = \sum_{K,\gamma} N_{K,\gamma} \frac{f(\rho)}{\rho^{5/2}} \mathcal{J}^{JM}_{K\gamma}(\Omega_\rho),$$
$$f(\rho) = \sqrt{7/5}(21\rho^{5/2}/\rho_0^3)\, \exp[-\sqrt{21/2}\,(\rho/\rho_0)]. \quad (5)$$

The function $f(\rho)$ is defined in such a way that it is normalized and its rms radius is defined by $\langle \rho \rangle = \rho_0$.

III. PROPERTIES OF THE SOURCES

To understand the continuum calculations of this work we need to illustrate the properties of the obtained source functions in details.

In our treatment of the reaction with ^{11}Li we assume the removal of the $p_{3/2}$ proton from the ^{9}Li core leading to the ^{8}He g.s. population. The integrated ^{10}He formfactors, as function of the momentum transfer q

$$|\Phi^{JM}_{q,\gamma,l_p}|^2 = \int d\Omega_q\, d^3X\, d^3Y\, |\Phi_{\mathbf{q}}(\mathbf{X}, \mathbf{Y})|^2, \qquad (6)$$

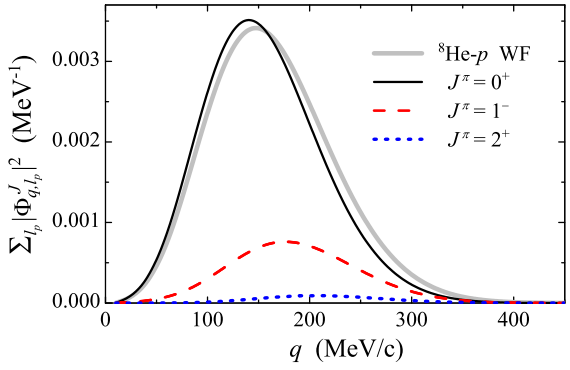

FIG. 2. Squared formfactors for population of different states in ^{10}He. Realistic ^{9}Li WF. The proton formfactor for ^{9}Li WF is shown for comparison by thick gray curve. It is scaled to match the normalization of the 0^+ formfactor.

are shown in Fig. 2. The formfactors are normalized as

$$\sum_{\gamma l_p} \int dq \, |\Phi^{JM}_{q,\gamma,l_p}|^2 = \frac{\pi}{2}, \qquad (7)$$

for ^{11}Li WF normalized to unity. The Fig. 2 provides the first idea about population of ^{10}He states with different J^π in our model: it is clear that beside 0^+ population we can expect a sizable population of the ^{10}He continuum with 1^- and 2^+ states. The momentum distribution of the 0^+ formfactor is very similar to initial formfactor of the ^{8}He-n motion, but for higher J^π there is a significant shift to higher momenta.

The correlation densities for the most important ^{10}He source functions are illustrated in Fig. 3. For the 0^+ state the correlation density is very similar to the one for the initial ^{11}Li WF (Fig. 3a) when we look on the bulk of the WF. In asymptotic regions significant differences can be seen.

The radial properties of source functions are illustrated in Fig. 4. One aspect of these properties is well expected: the size of the generated source is decreasing with the increase of the momentum transfer. In the limit of small momentum transfer the rms radius of the 0^+ source tend to that of initial ^{11}Li WF. This mean that in the first approximation the population of the ^{10}He g.s. can be considered as if it is happening directly from radial configurations of the ^{11}Li WF. It should be noted that with the increase of J the radial extent of the sources significantly grows, which lead to important consequences for the obtained excitation spectra of ^{10}He, see Fig. 5 and discussion in the Section 5.

In the proposed reaction model the ^{10}He recoil, the energy transfer into the ^{10}He system, and the ΔJ^π transfer to ^{10}He are taken to account. ΔJ^π should be mainly sensitive to two aspects of the structure: (i) the mass difference between the removed particle (proton) and the core of the final system (^{8}He), (ii) the relative size of the orbital motion of the removed particle and halo particles.

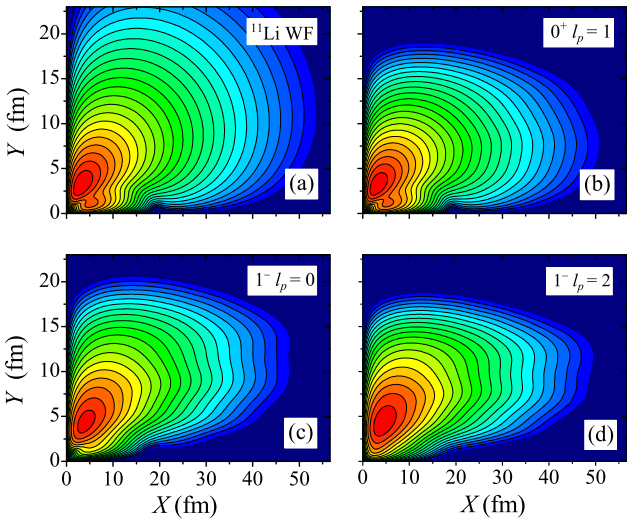

FIG. 3. Correlation densities for ^{11}Li g.s. WF (a) and for different source functions for ^{10}He (b,c,d). The q values chosen for different J^π correspond to peaks of the formfactors, see Fig. 2. The scale is four contours per order of the magnitude.

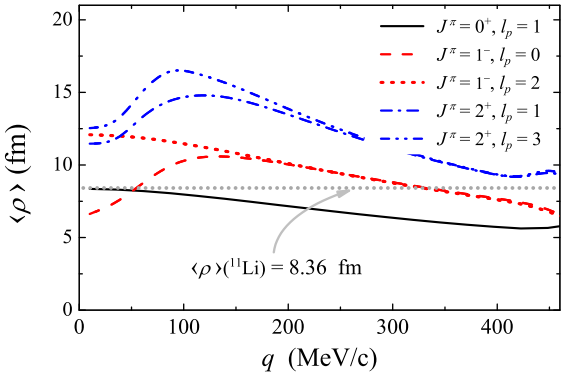

FIG. 4. Root mean square hyperradii for the source functions of different states in ^{10}He. The rms ρ value for the ^{11}Li WF is shown by gray dotted line.

Point (i) can be used for consistency checks: in the limit $M(^8\text{He}) \to \infty$ only the $J^\pi = 0^+$ source survives, while the others tend to zero. The actual scale of this trend is a such that for $M(^8\text{He}) \gtrsim 30 M_N$ the configuration with $J^\pi = 0^+$ is populated with 99% probability.

Point (ii) is illustrated in Fig. 5. These figures show excitation spectra of ^{10}He obtained by the Fourier transformation of sources obtained with ^{8}He-p relative motion WFs obtaining by variation of radial extent. Fig. 5(b) corresponds to realistic WF, while the (a) and (c) cases should demonstrate a possible variation scale. Such excitation spectra correspond to the physical situation of no FSI in the outgoing ^{10}He channel. This can be considered as an extreme test case of initial state structure effects on the observable ^{10}He properties. Following main features

of the distributions in Fig. 5 should be emphasized:

1. Even very large variation of the ^{11}Li radius leads to moderate variation in the ratio of different J^π population.

2. Population of higher J^π grows with asymmetry between the WF size of removed particle and in the WF size of the halo configuration of the ^{11}Li.

3. Population of higher J^π is never small. It can be expected up to 50% for the low-energy excitations of ^{10}He. However, there also could hardly be expected less than 20% of 1^- population.

4. Even *without any final state interaction* in the ^{10}He channel we can expect very low-energy response in the ^{10}He spectrum. It is actually peaked at *lower energy* than observed experimental peak in the spectrum of ^{10}He, see Fig. 7(c).

5. Excitations with higher J^π without FSI have profiles very similar to those of the 0^+ contribution with peaks mainly below $E_t \sim 2$ MeV of excitation in ^{10}He.

Having in mind this anomalous behavior of the sources, let's turn to ^{10}He dynamical three-body continuum calculations.

IV. SPECTRA OF ^{10}HE STATES

The spectrum of ^{10}He (0^+) is calculated with the source function Eq. (4), is shown in Fig. 6 as a function of the transferred momentum q. At very low transferred momentum, e.g. $q < 50$ MeV/c, the sanctum is very stable. With the increase q the spectrum shifts to considerably higher energy E_T: by ~ 250 keV for peak values and by ~ 1 MeV for q approximately 300 MeV/c. This effect should be taken into account thinking about more realistic reaction calculations. It is known that in the Glauber model the reaction is more peripheral and the momentum transfer is shifted towards the lower values. Thus some reduction in the E_T peak position can be expected compared to this calculation.

TABLE I. Source function properties for calculations of Fig. 5 obtained by variation of the radial size of WF in the ^{8}He-p channel. This variation was achieved by varying potential depth and thus the proton binding energy E_b. Probabilities for different J^π population are in percent.

case	$\langle r'_p \rangle$ (fm)	E_b (MeV)	$W(0^+)$	$W(1^-)$	$W(2^+)$
"Narrow"	2.0	-30.	66.3	27.6	6.2
Realistic	2.86	-13.93	79.2	18.5	2.3
"Broad"	3.5	-0.5	84.6	14.2	1.1

For conventional situation of nuclear reactions we expect the source size to be of the typical nuclear size [$\langle\rho\rangle = 3 - 5$ fm]. The calculation with the source Eq. (5) with such radii shown in Fig. 7 (a).

The situation changes drastically when we turn to the ^{11}Li source [see Fig. 7 (b)]. All three major configurations predicted to be populated $\{0^+, 1^-, 2^+\}$ are shifted now to extreme low energy $E_T \sim 1.3 - 1.6$ MeV. The overall picture is in a close analogy with what can be seen in Fig. 5 for calculations without any FSI. It is evident that the "momentum content" of the sources associated with nucleon removal from ^{11}Li is such low that the observed excitation spectrum is not significantly sensitive to the FSI any more and reflects predominantly the initial state structure. What especially attracts the attention here is that the states with different J^π (the 0^+, 1^-, and 2^+ configurations) are peaked at practically the same energy, which strongly contradicts typical expectations that they are separated by some MeVs.

Fig. 7 (c) provides a qualitative comparison of spectra provided by different models with two available data sets for proton removal from ^{11}Li [1, 5]. The Fourier transformation of the ^{11}Li WF provides the excitation spectrum for ^{10}He peaked at too low energy which immediately can be ruled out. The accounting for the reaction mechanism in our model but without FSI leads to the results much closer to experiment. The inclusion of FSIs bring us to a better agreement with the experiment. We should pay an attention here that the calculated effect of FSI is opposite to common expectation: the cumulative effect of the ^{10}He FSI is the shift of the spectrum to a higher energy and thus can been seen as an *effective repulsion*.

The reaction mechanism model considered in this work (sudden proton removal) can be considered as quite simplistic. However, we know that such an approach provides qualitatively correct results for majority of high-energy fragmentation reactions with exotic nuclei. Moreover, if a more realistic model (e.g., Glauber) is considered then the reaction becomes more peripheral. Our estimates indicate that in such a case the relative population of the 1^- state is enhanced. Thus our results could be considered as a conservative estimate of the proposed phenomenon of the anomalous ^{10}He spectrum population.

V. FSI VS. ISS RESPONSE IN ^{10}HE

After we realized the importance of the initial state contribution to the observable spectrum of ^{10}He populated from ^{11}Li it is natural to inquire: "Where is the borderline between a domination of final state interaction and an initial state contribution to the observables?" To answer this question we have performed systematic model calculations with sources of different radii. The results of these calculations are summarized in Fig. 8 providing the peak positions as a function of the source rms radius.

Let us have a look on the ^{10}He ground state behavior.

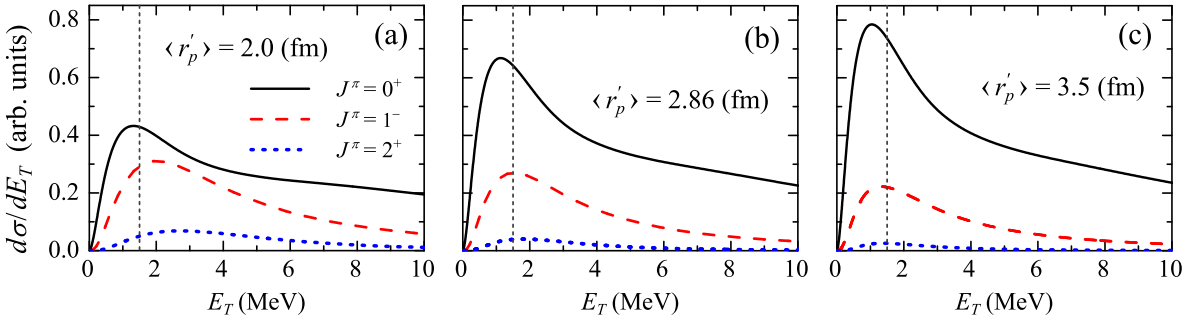

FIG. 5. Fourier transform for ^{10}He sources provides the excitation functions for 0^+, 1^-, and 2^+ in the approximation of no final state interactions. Different panels show the results obtained for different ^{8}He+p WFs. The calculations with realistic rms radius $\langle r_p' \rangle$ are given in panel (b), while the results of (a) and (c) demonstrates the possible scale of variation. Vertical dotted line at 1.5 MeV is shown to guide the eye.

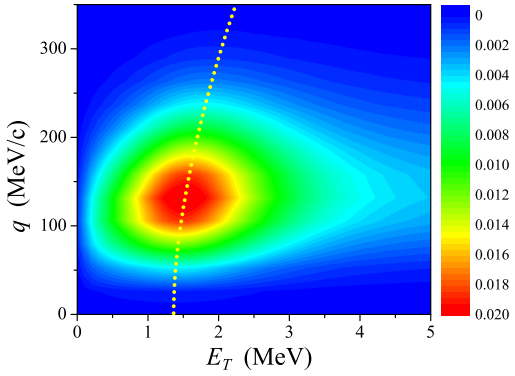

FIG. 6. Contour plot of the population cross section for ^{10}He 0^+ g.s. as function of the decay energy E_T and the transferred momentum q. The dotted curve is provided to guide the eye for position of the cross section peak as function of q.

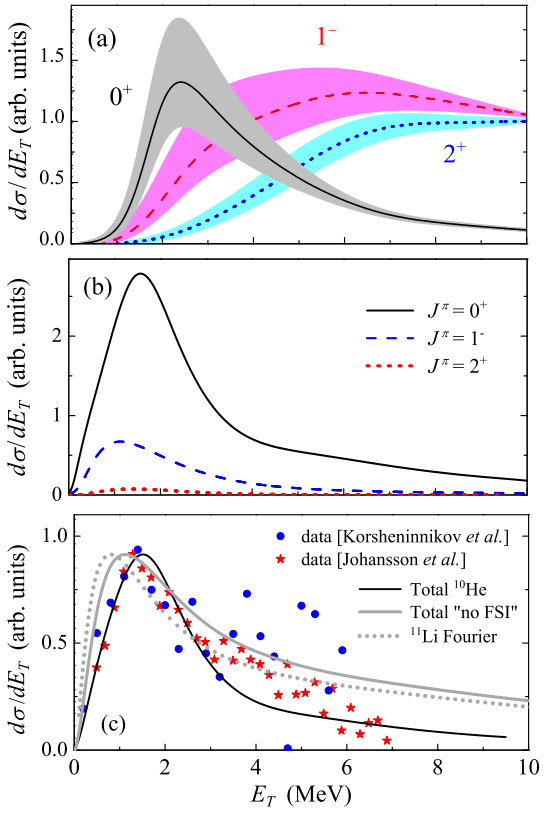

FIG. 7. The predicted spectra of states with different J^π. Panel (a) shows estimate results for "conventional" situation. Calculations for proton removal from ^{11}Li are given in panel (b). The total spectrum is qualitatively compared with experimental data [1, 5] in panel (c). Vertical dotted line at 2 MeV is shown to guide the eye.

For very small source radii the ground state is not well populated (the first peak in the cross section is found at high energy). However for $\langle\rho\rangle \sim 3-5$ fm the first peak position is relatively stable at about $2.5-2.0$ MeV. This energy well corresponds to the 0^+ resonance position defined in [10] via eigenphases for $3 \to 3$ scattering. With the source radius increase the 0^+ peak position continue to slide down. At about $\langle\rho\rangle \sim 9$ fm (for ^{11}Li $\langle\rho\rangle \sim 8.36$ fm) the FSI curve crosses with no FSI curve This probably should be interpreted in such a way that for such radial characteristics the low-energy response imposed by ISS can not be any more distinguished from the FSI effect in principle.

VI. "PILEUP" OF DIFFERENT STATES IN ^{10}HE

The Fig. 8 allows to understand qualitatively the picture of the "pileup" of states with different J^π, which is shown in Figs. 5 (b) and 7 (b) with and without FSI. The systematics for different states are very different in Figure 8. For the sources with very large radii both the FSI and no FSI curves crossed the line with $E_T = 1.5$ MeV decay energy at about 9, 11, and 14 fm for 0^+, 1^-,

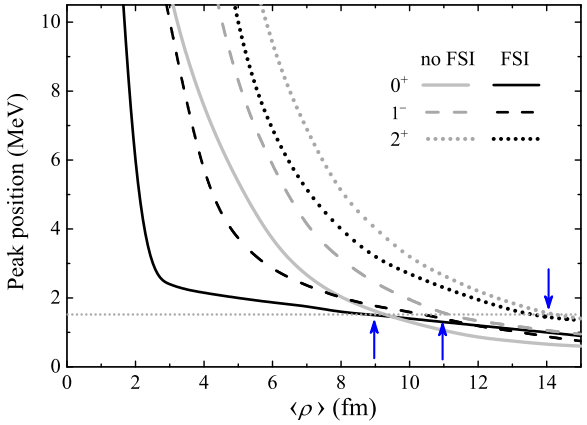

FIG. 8. Peak positions in the spectrum of ^{10}He for different J^π as function of the source root mean square hyperradius $\langle\rho\rangle$. Cases of FSI is shown by black lines and without FSI is shown by gray lines. Arrows mark $\langle\rho\rangle$ typical for sources with different J^π. Horizontal dotted line at 1.5 MeV is shown to guide the eye.

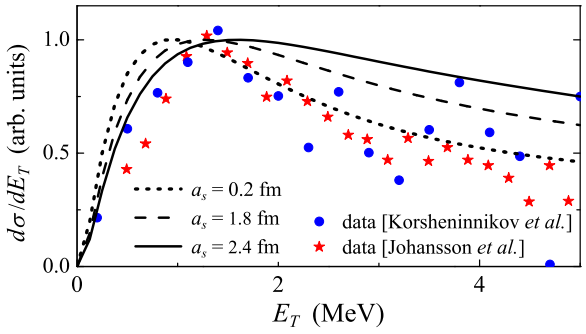

FIG. 9. Calculation with only s-wave interaction included in the ^{8}He-n channel. The interaction is characterized by the scattering length a_s as indicated in the legend.

and 2^+ states respectively (indicated by arrows). However, if we turn to Fig. 4 we find that the realistic sources for ^{10}He continuum population have very similar typical $\langle\rho\rangle$ values corresponding to the expected q values. They are about 7.8 fm at 140 MeV/c, 10.5 fm at 175 MeV/c, and 13.5 fm at 210 MeV/c for 0^+, 1^-, and 2^+ states respectively.

Thus the "pileup" of states with different J^π [Figs. 5b and 7b] obtained in our model at energy about 1.5 MeV can be obtained in a very simplistic model for the source of pure "geometrical" effect. The fact that the peaks of the responses with different J^π are found at about the same energy is connected to the systematic increase of the deduced source radii with the increase of J. This is in turn the effect of the removed recoil particle providing larger radial characteristics to terms of the source function with higher angular momentum.

VII. LIMITS ON THE ^{9}HE G.S.

Strong sensitivity of the observable ^{10}He spectrum to interactions in the ^{8}He-n channel was demonstrated in paper [10]. Exploratory studies of Ref. [10] were motivated by a variation in ^{9}He properties obtained in different experimental studies. Essential questions here were connected with intensity of the s-wave interaction, which was assumed to be a "strong" virtual state in some works (e.g. Ref. [14]), and properties of the lowest resonant state (presumably $p_{1/2}$), which in some works is assumed to have a very small, evidently not single-particle width (e.g. Ref. [15]). Since that time the new experimental results on ^{9}He spectrum continue to be controversial. On the one hand, it was found that there is no "strong" virtual state in ^{9}He [5, 16] providing the scattering lengths as $a_s \approx -3$ fm and $a_s \geq -3$ fm correspondingly. On the other hand a low-lying structure, corresponding to $a_s \approx -12 \pm 3$ fm was observed [17].

It should be understood that conclusions of *all* the experimental papers were based on the interpretations which were at the limit of the statistical reliability or/and the resolution of the corresponding data sets. Because we think that the reliability of the ^{10}He spectra obtained in the proton knockout from ^{11}Li is confirmed and our understanding of the reaction mechanism is generally reliable, we decided to reverse the problem and to check what are the limitations imposed by the ^{10}He spectrum on ^{9}He spectrum via the theoretical model calculations.

For example, to impose limits on the s-wave interactions in ^{8}He-n channel we make calculations with only s-wave interactions included in the three-body Hamiltonian, see Fig. 9.

The limiting value of the scattering length we define, at the moment, when the ground state peak goes below about 1 MeV, which make it clearly inconsistent with the data.

If we make such a procedure systematically (requesting the peak position to be not lower then 1 MeV) also for the p-wave interactions, then the constrains on the plane of s-wave vs. p-wave interaction parameters can be derived, see Fig. 10. We can see that practically none of the available experimental data are consistent with these constrains. The constrains given in Fig. 10 are, of course, relevant by the nature of our model only to the single-particle states. However, it is evident that anyhow fully conclusive experimental studies of ^{9}He with convincing statistics, sufficient energy resolution, and clear spin parity identification of the states are required.

VIII. THREE-BODY CORRELATIONS

The importance of the initial state and recoil effects was clear to the authors of Ref. [18], where ^{10}He was populated in the proton knockout from ^{11}Li. They even provide some qualitative estimates of the expected effects.

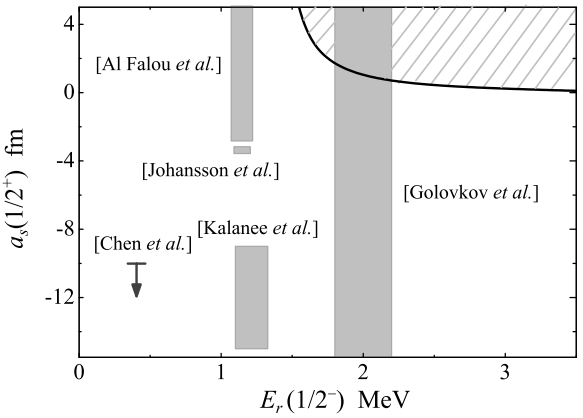

FIG. 10. Limits on the s-wave $1/2^+$ and p-wave $1/2^-$ interactions in ^{9}He (^{8}He+n channel). a_s is the s-wave scattering length and E_r is the $1/2^-$ resonance energy. Hatched area shows the region admissible according to our calculations. Gray rectangles show experimentally obtained limits for ^{8}He+n interactions. Experiment [14] gives only the limit for scattering length. So it is displayed as the arrow.

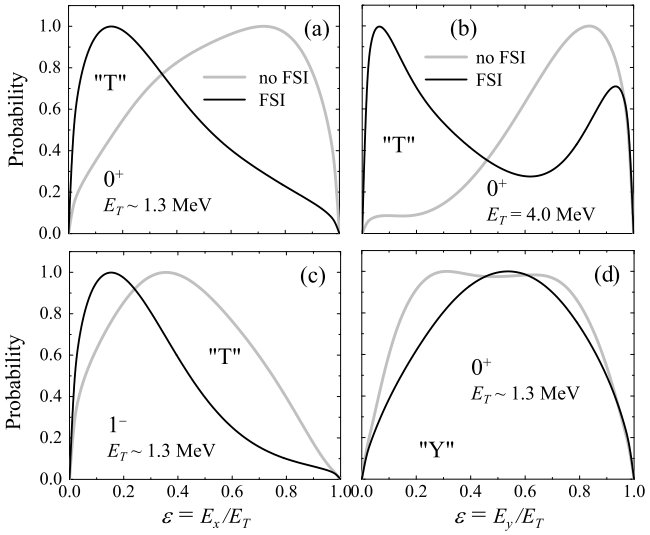

FIG. 11. Different energy correlations for ^{10}He populated in proton knockout from ^{11}Li. Calculations with and without FSI are shown by black and gray curves. (a) 0^+ state, Jacobi "T" system, the energy corresponds to the peak value of each distribution. (b) 0^+ state, Jacobi "T" system, $E_T = 4$ MeV. (c) 1^- state, Jacobi "T" system, energy as in panel (a). (d) 0^+ state, Jacobi "Y" system, energy as in panels (a) and (c).

They suggested a possible "workaround" for this problem. It was shown in [18] that the three-body correlation patterns observed for the low-energy peak in ^{10}He spectrum are different from the correlations inherent from the momentum correlations of ^{11}Li WF. This fact was interpreted in such a way, that this peak is not a remnant of initial ^{11}Li state, but a true dynamical formation and thus a ^{10}He ground state.

Let us have a look what we get here with much more precise treatment of reaction mechanism and correct accounting for the ^{10}He FSIs. Energy distributions between nucleons are typically most sensitive to decay dynamics. Fig. 11 (a) show this distribution for the peak energy of the 0^+ spectrum. The distributions calculated *with* and *without* FSI demonstrate totally different pictures. The "no FSI" distribution is quite close to the momentum distribution in ^{11}Li (also shown in [18]). However, the full calculation shows a kind of "opposite" correlation, evidently dominated by attractive neutron-neutron contribution. Fig. 11 (d) shows also the correlations in the core-neutron channel. The difference between no FSI and FSI cases is not so spectacular here, but still quite sizable.

Because the energy spectra calculated *with* and *without* FSI are very close to each other we arrive to important conclusion about decay dynamics for this case. In conditions of the powerful ISS effect connected with ^{11}Li, the ^{10}He FSI is not sufficiently strong to modify total excitation spectrum. However, it is sufficiently strong to rearrange the correlation patterns. Thus the spectrum shape is based mainly on ISS, while the three-body correlations are FSI dominated.

The energy range around 4 MeV was assigned to 2^+ state in Ref. [18]. Important reason for that was the observed change in the correlation pattern compared to those in the $1-3$ MeV energy range. In our calculations we found the 2^+ contribution small and focused at small energies. In Fig. 11 (b) we demonstrate the distributions connected with the same 0^+ excitation but at $E_T = 4$ MeV. Again, as in Fig. 11 (a) there is a strong difference between no FSI and FSI result. There is also a strong difference with the FSI distributions of Fig. 11 (a) and (b) calculated for the same J^π. The variation of the energy distributions Fig. 11 (a,b) with energy is therefore not a good indicator for the change in the J^π. There are an examples, where the problem of the using the three-body correlations to spin-parity identification was successfully solved. In Refs. [6, 19] this was done for ^{5}H and ^{10}He systems. However, this requires treatment of more complicated (5-dimensional in general case) correlations connected with orientation of the three-body system as a whole.

The calculated full distribution in Fig. 11 (a) is in a reasonable agreement with the spectrum from [18]. Unfortunately the direct quantitative comparison is not possible here because of complicated corrections connected with experimental setup. Note, that in conditions of "J^π pileup" discovered in this work the interference with the sizable 1^- contribution may become important. It has been shown in [20] how the three-body correlation patterns become sensitive to the interference conditions and experimental bias. The correlations for the 1^- state by itself are given in Fig. 11 (c). The demonstrated energy correlations in n-n channel is similar to the energy correlations for the 0^+ state. They demonstrate the similar

type of the no FSI vs. FSI behavior as the 0^+ state.

The calculations of this Section demonstrates that conclusions about ^{10}He spectrum obtained in Ref. [18] on the basis of correlations using only speculative argumentation not supported by theoretical studies are not valid.

IX. ORIGIN OF THE 1^- EXCITATION

The evidence for the low-lying 1^- state in ^{10}He was obtained in paper [6] in the ^{8}He(t,p) reaction. It is based on the observation of asymmetry of the angular distributions of ^{8}He fragment in the ^{10}He c.m. frame for ^{10}He excitation energies $E_T = 4-6$ MeV. It was demonstrated in [6] that such a 1^- state position is consistent with the trend along $N = 8$ isotone defined by the shell structure breakdown in ^{12}Be. The results of Ref. [6] concerning 1^- state were questioned in the paper [21] basing on argumentation mainly connected the data treatment and analysis procedures of Ref. [6].

We can comment on the controversy between ideas of [6] and [21] about excited states of ^{10}He. All the structures predicted here for the spectrum of ^{10}He are quite broad. So, we immediately can expect strong sensitivity to population mechanism. From Fig. 8 we can learn that for 1^- and 2^+ states the sensitivity just to one aspect of reaction mechanism (modeled by the radial size of the source function) is so strong that it totally overshadows the predicted effect of the FSI. Such structures can not be interpreted as resonant states (which major properties are independent on the population mechanism) and should be attributed to so-called "soft" excitations (which appearance is impossible without specific population mechanism).

To gain a deeper understanding of the situation we provide in Fig. 12 selected cases of the spectra used in Figure 8. The partial wave decomposition shows that the 1^- spectra are always dominated by two components of hyperspherical decomposition: $K = 1$ and $K = 3$. It can be shown that in the shell-model-like picture $K = 1$ component can be identified with $[sp]$ configuration, while $K = 3$ is closely related to $[dp]$. The low-energy part of spectrum is always connected with $[sp]$ configuration. In such a configuration one particle is in resonance (p-wave) and one in non-resonant (s-wave), so this is real "soft" excitation totally depending on initial configuration. In contrast, for the $[dp]$ configuration resonant behavior could be expected in principle (based on the p- and d-wave states of ^{9}He), but do not really show up in calculations. The profiles for population of the $[sp]$ and $[dp]$ configurations are very different for different calculations. While for experimental conditions of Ref. [5] practically only $[sp]$ configuration is expected to contribute the spectrum, for conditions of Ref. [6] the large mixing of configurations is predicted.

Our message here is that not only it is very probable to expect strong population of 1^- continuum at $E_T = 4-6$ MeV in experiment [6], it is also likely that the data [5] of the Authors of Ref. [21] itself contains important 1^- contributions. We should remind here again that our conclusions are valid only for the ^{10}He states "built" on the single-particle structures of ^{9}He subsystem.

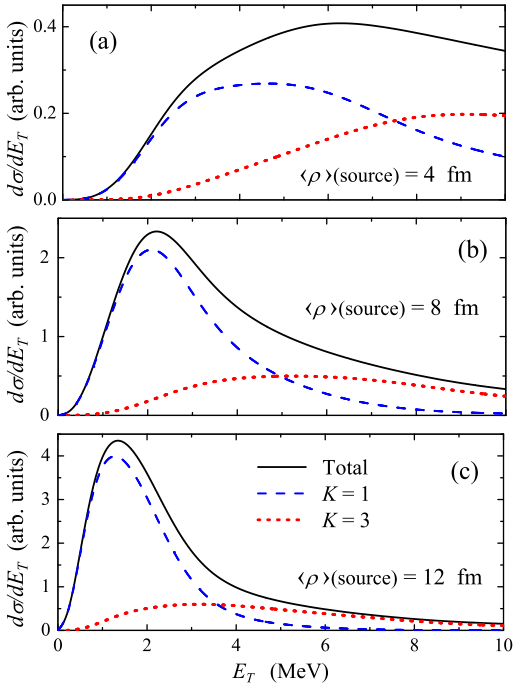

FIG. 12. Spectra of 1^- excitations obtained for different radii of source functions $\langle r\rangle = 4$, 8, and 12 fm are shown in panels (a), (b), and (c) correspondingly. The contributions of the dominant $K = 1$ and $K = 3$ configurations are given by dashed and dotted curves.

X. ^{10}HE PRODUCTION IN REACTIONS WITH ^{14}BE

A novel way to populate ^{10}He was used in the recent work [7]. The ^{8}He+n+n invariant mass was reconstructed for ^{14}Be beam reaction on the light target. The ^{10}He spectrum well coincide (within errorbars) with the spectra [1, 5]. However, somewhat different properties of ^{10}He g.s. are inferred with $E_T = 1.6(0.25)$, $\Gamma = 1.8(4)$ MeV. This experiment, presented by the Authors as the "two-proton removal" has two most probable interpretations. One interpretation is the two-proton knockout populating continuum of ^{12}He system. Broad continuum states of the unknown ^{12}He are then decaying "sequentially" populating the ^{10}He ground state. Alternative opportunity, which we also find very probable, is the α knockout.

Let's discuss the second opportunity. The α knockout from ^{14}Be can be treated in the same model as we applied for the knockout from ^{11}Li. We then ^{12}Be is considered as a core for ^{14}Be. This is not an extremely well defined core, however we can find the ^{14}Be three-body

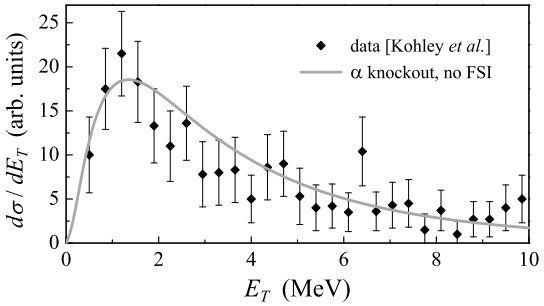

FIG. 13. "No FSI" estimate for the ^{10}He spectrum populated in α knockout from ^{14}Be. The $q = 100$ MeV/c value is selected.

^{12}Be+n+n WF in the literature [22]. The ^{12}Be core we consider as a ^{8}He+α system in a potential model providing a reasonable size and correct separation energy for alpha particle. The estimates without FSI shown in Fig. 13, demonstrate a qualitative agreement with the data and indicate that the large ISS effect analogous to that in ^{11}Li case can be taking place in the case of the halo structure of ^{14}Be. It seems that the more sophisticated calculations are not necessary at the moment until the experimental situation becomes more definite.

XI. CONCLUSIONS

We would like to emphasize the following main results of this work

(i) The calculations of this work indicate that a "ground state" peak observed in the spectrum of ^{10}He populated in reactions with ^{11}Li is likely to be a superposition of 1^-, 0^+, and 2^+ states. The calculated effect could be seen as one of the most powerful indications of the abnormal halo size of ^{11}Li nucleus.

(ii) "Pileup" of 1^-, 0^+, and 2^+ states obtained in the calculations of this work is a consequence of the systematic increase of the radial sizes of sources with J. This is, in a row, consequence of the core recoil effect in the case of expressed halo structure.

(iii) The energy transfer to ^{10}He is small in all considered model assumption if ^{11}Li WF as initial state is involved. In contrast, the angular momentum transfer to ^{10}He considerably depends on the properties of ^{11}Li WF.

(iv) The actual lowest excitation in the ^{10}He spectrum is predicted to be "soft" 1^- peak, created by an extreme spatial extent of the initial state configuration (^{11}Li halo nucleus). This is an extremely exotic situation having no match so far in the other systems and reactions.

(v) The strong initial state effect could be a generic problem for reactions populating broad states of $2n$ emitting systems beyond the driplines. We can mention here recently measured ^{13}Li populated in the proton knockout off ^{14}Be [5] and ^{16}Be populated in the proton knockout off ^{17}B [23].

(vi) Our calculation result reconcile the experimental results obtained in the knockout reactions on halo systems [1, 5, 7] with the data from the (t,p) transfer reaction [4, 6]. In our interpretation there is no problem with any of these data by itself, but the interpretations should be very different. This new interpretation prescribe "new" ground state position for ^{10}He ~ 2.1 MeV [6] compared to value ~ 1.3 MeV accepted since discovery of ^{10}He [1].

(vii) The data on ^{10}He spectrum can be used to impose constrains on the spectrum of ^{9}He. These constrains are valid under the assumption of a single-particle nature of the low-lying states of ^{9}He. Within this assumption we see that practically all the data on the ^{9}He $1/2^+$ and $1/2^-$ states are incompatible with the ^{10}He data discussed in this work.

(viii) Three-body correlation studies further clarifies the role of the final state interaction in the situations discussed here. We have found in this work that the ^{10}He FSI is insufficiently strong to modify the excitation spectrum, governed thus by the initial state structure. However, it is strong enough to completely rebuild the correlations patterns of the fragments.

Situation with the studies of the ^{10}He g.s. which we address in this work underline the importance of the theoretical studies in interpretation of complex and unusual phenomena in the exotic dripline systems. Our results also call for deeper and finally more conclusive experimental studies of ^{10}He system. Such studies should make ^{10}He benchmark system and basis for understanding of the two-neutron emitters beyond the dripline.

Acknowledgments. — The work was carried out with the financial support of SAEC "Rosatom" and Helmholtz Association. L.V.G. is supported by RFBR 11-02-00657-a grant and Russian Ministry of Industry and Science grant NSh-932.2014.2.

[1] A.A. Korsheninnikov *et al.*, Phys. Lett. **B326**, 31 (1994).
[2] A.N. Ostrowski *et al.*, Phys. Lett. **B338**, 13 (1994).
[3] T. Kobayashi *et al.*, Nucl. Phys. **A616**, 223c (1997).
[4] M.S. Golovkov *et al.*, Phys. Lett. **B672**, 22 (2009).
[5] H.T. Johansson *et al.*, Nucl. Phys. **A842**, 15 (2010).
[6] S.I. Sidorchuk *et al.*, Phys. Rev. Lett. **108**, 202502 (2012).
[7] Z. Kohley *et al.*, Phys. Rev. Lett. **109**, 232501 (2012).
[8] S. Aoyama, Phys. Rev. Lett. **89**, 052501 (2002).
[9] A. Volya and V. Zelevinsky Phys. Rev. C **74**, 064314 (2006).
[10] L.V. Grigorenko and M.V. Zhukov, Phys. Rev. C **77**, 034611 (2008).
[11] M.S. Golovkov *et al.*, Phys. Rev. C **76**, 021605(R) (2007).
[12] N.B. Shulgina, B. Jonson, M.V. Zhukov, Nucl. Phys. **A825**, 175 (2009).
[13] J. Raynal and J. Revai, Nuovo Cimento **A68**, 612 (1970).

[14] L. Chen *et al.*, Phys. Lett. B **505**, 21 (2001).
[15] H.G. Bohlen *et al.*, Prog. Part. Nucl. Phys. **42**, 17 (1999).
[16] H. Al Falou, A. Leprince, and N.A. Orr, J. Phys.: Conf. Ser. **312**, 092012 (2011).
[17] T. Al Kalanee *et al.*, Phys. Rev. C **88**, 034301 (2013).
[18] H.T. Johansson *et al.*, Nucl. Phys. **A847**, 66 (2010).
[19] M. S. Golovkov *et al.*, Phys. Rev. C **72**, 064612 (2005).
[20] L.V. Grigorenko, I.A. Egorova, R.J. Charity, M.V. Zhukov Phys. Rev. C **86**, 061602 (2012)
[21] L.V. Chulkov, T. Aumann, B. Jonson, T. Nilsson, H. Simon, Phys. Lett. B **720**, 344 (2013).
[22] C. Forssen, V.D. Efros, M.V. Zhukov, Nucl. Phys. **A706**, 48 (2002).
[23] A. Spyrou *et al.*, Phys. Rev. Lett. **108**, 102501 (2012).